

## Electron-Atom Shadow Scattering

Jürgen Geiger and Dagoberto Morón-León<sup>(a)</sup>*Fachbereich Physik, Universität Kaiserslautern, D 6750 Kaiserslautern, Federal Republic of Germany*

(Received 26 February 1979)

The elastic small-angle scattering of 15- to 25-keV electrons by He, Ne, and Ar shows a rapid increase towards decreasing scattering angles superimposed with a diffraction pattern. The observed excess of the elastic differential cross section as compared with the Born cross section is due to the coupling to the inelastic channels. It may be also explained as a diffraction into the shadow of the inelastic scattering which dominates the forward direction.

It has been well known for a long time (see Mott and Massey)<sup>1</sup> that the differential cross section for the elastic scattering of low- and medium-energy electrons (below 1000 eV) at small scattering angles exceeds that given in first Born approximation. A summary of the experimental work on the rare gases was given by Bromberg in his papers<sup>2, 3</sup> on absolute differential cross sections.

A first attempt to explain these deviations at small scattering angles was due to Massey and Mohr.<sup>4</sup> They include the influence of the inelastic channels on the elastic scattering in a second Born approximation. Their calculation led to a complex expression from which a contribution could be separated having the nature of an effective polarization potential acting on the incident electron. This is the way along which the electron-scattering experiments have mostly to be interpreted: deformation of the electronic charge cloud under the influence of the incoming electron. This charge-polarization effect is commonly believed to be at least small for keV electrons and the Born approximation is believed to be valid in the limit of vanishing momentum transfer.

In a paper,<sup>5</sup> to which less attention has been paid hitherto, Mohr studied the channel-coupling effects on the elastic scattering from atomic hydrogen by a partial-wave analysis and came to a quite different conclusion. He found that even for 34-keV electrons an elastic forward peak still exists with a half width of a few tenths of a degree. The aim of the present experiment is to resolve this contradiction.

Figure 1 shows the experimental arrangement. The length of the collision chamber was 6 mm and the pressure in it was  $p_{\text{He}} = 2$  Torr,  $p_{\text{Ne}} = 0.1$  Torr, and  $p_{\text{Ar}} = 0.08$  Torr. The intermediate-image filter lens<sup>6</sup> forms an image of the demagnified electron source (diameter  $8 \mu\text{m}$ ) at the final screen (photographic plate) without altering its size. Electrons which have lost more than 8 eV energy are reflected by the filter lens. Each

measurement was followed by a test run without a target gas in order to subtract the stray background (5 to 20%). The angular range measured was between 0.4 and 7.5 mrad and continued earlier measurements<sup>7, 8</sup> with higher precision towards smaller scattering angles.

The results of the measurements are presented in Figs. 2-4, and the curves drawn through the data points should be understood as guides for the eyes. The Born elastic differential cross section, which is almost flat in this angular range, is also shown for comparison. The angular distributions were plotted in such a way that the outermost data points agree with the Born cross

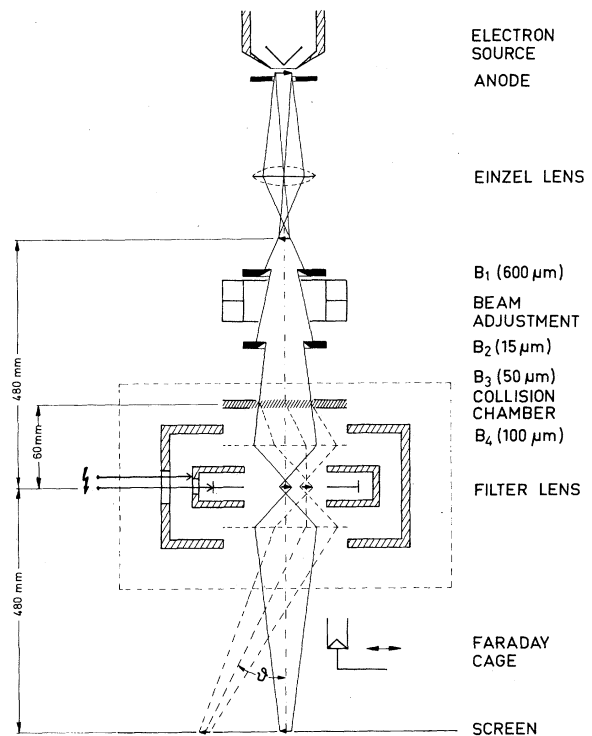


FIG. 1. Schema of the scattering apparatus and trajectory of rays.

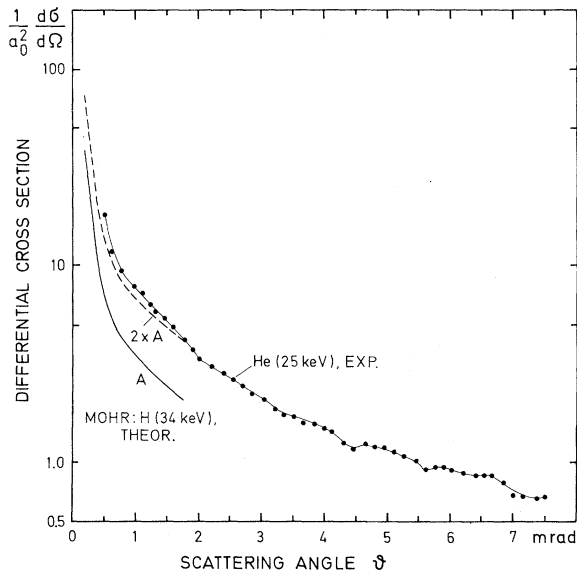


FIG. 2. Angular distribution of the elastically scattered electrons (25 keV) by helium. The elastic differential cross section for hydrogen and 34-keV electrons as calculated by Mohr (Ref. 5) is also shown.

section. This normalization is not exact, but earlier measurements<sup>8</sup> showed that this should be a reasonable estimate. The general behavior of all the distributions measured is the same: a strong increase towards smaller scattering angles. This increase seems to be steeper and concentrated to a narrower angular range the higher the energy of the electrons. Furthermore, the angular distributions exhibit distinct diffraction effects, most impressive for 15-keV electrons.

The channel-coupling calculation for hydrogen by Mohr<sup>5</sup> does not show any diffraction effects, nevertheless the computed differential cross section has quite the same tendency as the experimental results for helium, where the structure is rather weak (Fig. 2). On multiplying the theoretical distribution by an arbitrary factor of 2 this comparison is made more convenient. The diffraction effect discovered in the present study can be understood in terms of "shadow scattering." Shadow scattering was first introduced into atomic collision physics by Bethe.<sup>9,10</sup> For our purpose Fig. 1 of Ref. 7, which displays the differential cross sections for the scattering of 25-keV electrons by helium between  $10^{-2}$  and  $10^2$  mrad, will help to illustrate the following considerations.

The total scattering of electrons into angles

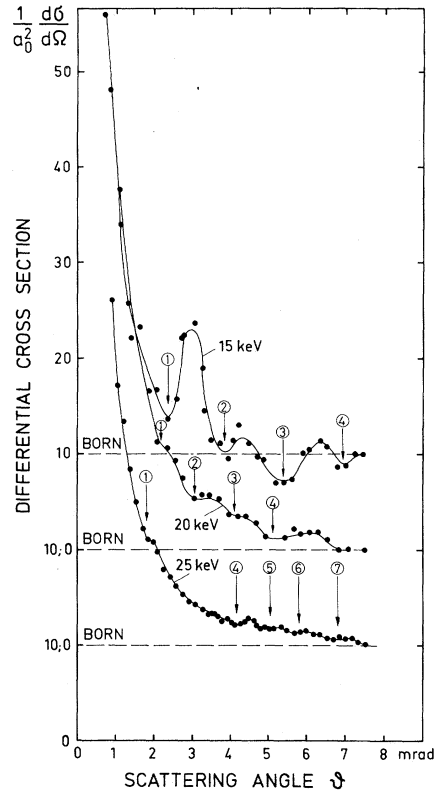


FIG. 3. Angular distribution of the elastically scattered electrons by neon. The Born cross section (dashed line) is independent of energy in this angular range, and the curves are displaced against each other. The figures at the arrows give the order of the diffraction minima (see Table I).

smaller than about 10 mrad is dominated by inelastic processes—the maximum differential cross section is due to the excitation of the resonance line. The ratio of the inelastic to the elastic differential cross section at zero scattering angle is of the order of  $\alpha_0^2 k_0^2$ , where  $k_0$  is the wave number of the primary electrons and  $\alpha_0$  the Bohr radius. This ratio amounts to as much as  $2 \times 10^3$  for 25-keV electrons. Thus for sufficiently small scattering angles almost all electrons are scattered inelastically, and behind the filter lens, which is impervious to these electrons, the atom looks like a black circular disk. This disk must in turn give rise to a diffraction pattern. The radius of the disk can be derived by regarding the angular distribution of the inelastically scattered electrons as a zeroth-order diffraction maximum with half the half-width  $\vartheta_E = E/2E_0$ .  $E$  is the energy loss due to excitation of the resonance line and  $E_0$  the primary electron energy.

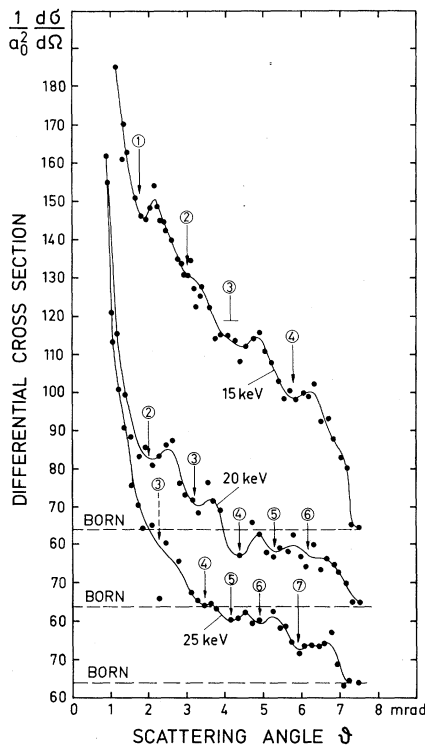


FIG. 4. The same as Fig. 3 for argon.

The radius is then given by

$$R = (k_0 \vartheta_E)^{-1}. \tag{1}$$

Note that the radius of our hypothetical disk depends on the energy of the incident electrons.

According to Fraunhofer diffraction theory<sup>11</sup> the angular positions of the diffraction minima are obtained from

$$\vartheta = n c_n \lambda / R = 2 \pi n c_n E m \lambda^2 / h^2, \tag{2}$$

provided the diffraction angle is small.  $n$  denotes the order of the diffraction minimum,  $c_n$  a number between  $c_1 = 0.61$  and  $c_7 = 0.52$  depending on the order  $n$ , and  $m$  and  $\lambda$  the mass of the electron and its wavelength, respectively. The diffraction minima rather than the maxima have been chosen since they are easier to identify. Their positions vary with the square of the electron wavelength and are labeled with the number of the diffraction order  $n$  in Fig. 3 and 4. Table I shows a comparison of the results for Ne and Ar: the scattering angles for the diffraction minima, the radii of the apparent atomic disk calculated from the diffraction pattern using Eq. (2), and the radii following from Eq. (1). The agreement between calculated and measured radii is surprisingly good. By the way, the dips in the angular distribution of heli-

TABLE I. Measured angles of diffraction minima  $\vartheta$  and the corresponding radii  $R$  of the apparent atomic disk according Eq. (2) for Ne and Ar. The radii,  $R$ (calc.), calculated by using Eq. (1) and the energy losses  $E = 16.9$  eV for Ne and  $E = 11.7$  eV for Ar, are also given for comparison.

N E O N						
n	25 keV		20 keV		15 keV	
	$\vartheta$ mrad	$R/\text{\AA}$	$\vartheta$ mrad	$R/\text{\AA}$	$\vartheta$ mrad	$R/\text{\AA}$
1	1.76	26.7	2.00	26.2	2.04	30.0
2			3.05	31.6	3.82	29.3
3			3.95	35.3	5.38	30.2
4	4.12	39.6	5.20	35.1	6.93	30.6
5	4.95	41.2				
6	5.70	42.9				
7	6.60	42.3				
$R$		38.6		32.0		30.0
$R$ (calc.)		38		34		30

A R G O N						
n	25 keV		20 keV		15 keV	
	$\vartheta$ mrad	$R/\text{\AA}$	$\vartheta$ mrad	$R/\text{\AA}$	$\vartheta$ mrad	$R/\text{\AA}$
1					1.75	34.9
2			2.05	47.0	2.90	38.6
3			3.25	42.9	4.10	39.5
4	3.40	48.0	4.31	42.3	5.70	36.9
5	4.03	50.6	5.31	42.9		
6	4.81	50.9	5.94	46.1		
7	5.87	47.9				
$R$		49.4		44.2		37.5
$R$ (calc.)		51		45		39

um fit also the model with  $R = 29 \text{\AA}$  obtained from  $E = 21.22$  eV. The model could still be refined by choosing a weak sphere with a partly penetrable surface layer instead of the circular disk.

From the point of view of the present work the anomalous behavior of the differential cross section of helium reported by Bromberg<sup>3</sup> appears quite normal: Because of its low atomic number, inelastic scattering compared to elastic scattering is exceptionally strong (see, e.g., Ref. 7). This circumstance will cause the shoulder of the shadow scattering to surpass  $2^\circ$ , Bromberg's low angular limit at electron energies below 700 eV. With increasing energy the shadow scattering is confined to smaller angles beyond the angular range of his apparatus and agreement with the Born cross section is obtained. For the heavier

rare-gas atoms the situation is invalid throughout for the electron energies applied (Ref. 10, page 243).

The authors thank R. A. Bonham, Bloomington, M. Inokuti, Argonne National Laboratories, and H. Krüger, Kaiserslautern, for valuable discussions. A grant from the Deutscher Akademischer Austauschdienst is gratefully acknowledged. This Letter was a part of a thesis submitted by one of us (D.M.-L.)

<sup>(a)</sup>Permanent address: Departamento de Física, Universidad del Valle, Cali, Colombia.

<sup>1</sup>N. F. Mott and H. S. W. Massey, *The Theory of Atomic Collisions* (Oxford Univ. Press, London, 1949),

2nd ed., especially p. 220.

<sup>2</sup>J. P. Bromberg, *J. Chem. Phys.* **50**, 3906 (1969).

<sup>3</sup>J. P. Bromberg, *J. Chem. Phys.* **61**, 963 (1974).

<sup>4</sup>H. S. W. Massey and C. B. O. Mohr, *Proc. Roy. Soc. London, Ser. A* **146**, 880 (1934).

<sup>5</sup>C. B. O. Mohr, *J. Phys. B: At. Mol. Phys.* **2**, 166 (1969).

<sup>6</sup>J. A. Simpson, *Rev. Sci. Instrum.* **32**, 1283 (1961).

<sup>7</sup>J. Geiger, *Z. Phys.* **175**, 530 (1963).

<sup>8</sup>J. Geiger, *Z. Phys.* **177**, 138 (1964).

<sup>9</sup>H. A. Bethe, in *Preludes in Theoretical Physics*, edited by A. de Shalit, H. Feshbach, and L. van Hove (North-Holland, Amsterdam, 1966), p. 241; see also J. M. Blatt and V. F. Weisskopf, *Theoretical Nuclear Physics* (Wiley, New York, 1952), p. 324.

<sup>10</sup>H. A. Bethe and R. Jackiw, *Intermediate Quantum Mechanics* (Benjamin, New York, 1968), p. 268.

<sup>11</sup>M. Born and E. Wolf, *Principle of Optics* (Pergamon, Oxford, 1970), 4th ed., p. 395.

## Irreversible Ponderomotive Effects in a Plasma

Hans Schamel

*Theoretical Physics I, Ruhr-University Bochum, D-4630 Bochum, Federal Republic of Germany*

(Received 12 March 1979)

A kinetic description is presented of ponderomotive effects which originate from a time-dependent high-frequency (hf) field. The solution of the corresponding generalized diffusion equation shows the appearance of a nonlocal term which reflects a memory of the plasma. It leads to significant changes of the plasma properties during and after the duration of the hf field. The plasma is irreversibly heated and a region of high density and high temperature appears at the center of hf activity in the time asymptotic limit.

The concept of ponderomotive force,<sup>1</sup> the simplest effect of high-frequency (hf) waves on slow plasma motion, is proven to be applicable in laser fusion and magnetic confinement. Profile modification, parametric instability, hf end plugging, etc., are pronounced examples of its usefulness. Recent progress<sup>2,3</sup> has revived interest in this phenomenon as more details of the general ponderomotive effect have been figured out. The objective of this Letter is to bring attention to another effect which arises from the transient nature of the hf waves. Time variation of the hf fields is, in fact, unavoidable in any realistic experiment. Some of the reasons are the turning on and the switching off of the external pump, internal dynamics (soliton-flash), or dissipation and convection of the hf waves.

I investigate the long-term behavior of the plasma electrons which react passively to a hf longi-

tudinal field. The analysis is based on the one-dimensional Vlasov equation

$$Lf = [E \exp(-it) + \text{c.c.}] \partial_v f, \quad (1)$$

where the Vlasov operator  $L$  is given by

$$L = \partial_t + v \partial_x + \varphi' \partial_v. \quad (2)$$

The notation and normalization are standard. The ambipolar field  $\varphi'(x, t)$  and the amplitude of the superimposed hf longitudinal field  $E(x, t)$  are assumed to be slowly varying functions of  $x$  and  $t$ . The perturbative treatment of (1), used as usual, demands both quantities to be small. Resonant particle effects are thus negligible. Then application of the method of characteristics leads to the following generalized diffusion equation

$$L\bar{f} = \psi' \partial_v \bar{f} + (\psi + v\psi') \partial_v^2 \bar{f} + 2\psi \partial_v L \partial_v \bar{f}. \quad (3)$$

Here  $\bar{f}$  includes the second-order distribution,